Retrieving 2-D Leaf Angle Distributions for Deciduous Trees From Terrestrial Laser Scanner Data

Article *in* IEEE Transactions on Geoscience and Remote Sensing · June 2018

DOI: 10.1109/TGRS.2018.2843382

5 authors, including:

Yumei Li
Chinese Academy of Sciences
10 PUBLICATIONS **75** CITATIONS
SEE PROFILE

Yanjun Su
Chinese Academy of Sciences
43 PUBLICATIONS **318** CITATIONS
SEE PROFILE

Tianyu Hu
Chinese Academy of Sciences
20 PUBLICATIONS **114** CITATIONS
SEE PROFILE

Guangcai Xu
Chinese Academy of Sciences
16 PUBLICATIONS **110** CITATIONS
SEE PROFILE

Retrieving 2-D Leaf Angle Distributions for Deciduous Trees From Terrestrial Laser Scanner Data

Yumei Li, Yanjun Su, Tianyu Hu, Guangcai Xu, and Qinghua Guo

***Abstract*— Terrestrial laser scanning is a promising tool for estimating leaf angle (including leaf inclination and azimuthal angles) distribution (LAD). However, previous studies focus on the retrieval of leaf inclination angle distribution, very few studies have considered the distribution of leaf azimuthal angle due to the restriction of measurement techniques. In this paper, we developed a new method to obtain more accurate leaf inclination and azimuthal angle estimations based on leaf point cloud segmentation and filtration and then fit LAD functions using two-parameter Beta-distribution model. In addition, we constructed a new projection coefficient model with two parameters $G(\theta, \varphi)$ using Nilson's algorithm based on the accurate retrieval of LAD. To assess the influence of leaf numbers on leaf inclination and azimuthal angle estimations, we modeled 160 individual leaves and 10 trees with different leaf numbers. In addition, to validate the final results, we also sampled three magnolia trees with different leaf numbers and manually measured leaf inclination and azimuthal angles of all their leaves using an angle measurement device. All results showed that the method proposed in this paper can provide accurate leaf inclination and azimuthal angles (leaf inclination angle: $R^2 = 0.98$, RMSE $= 2.41^\circ$ and leaf azimuthal angle: $R^2 = 0.99$, RMSE $= 3.44^\circ$). The simulated LAD and $G(\theta, \varphi)$ estimations based on these leaf inclination and azimuthal angles were strongly correlated with those obtained from ground truth measurements ($P > 0.05$).**

***Index Terms*— Beta-distribution model, leaf azimuthal angle, leaf inclination angle, projection coefficient model, terrestrial laser scanner (TLS).**

Manuscript received January 25, 2018; revised April 8, 2018 and May 23, 2018; accepted May 25, 2018. This work was supported in part by the National Key R&D Program of China under Grant 2017YFC0503905 and Grant 2016YFC0500202, in part by the Frontier Science Key Programs of the Chinese Academy of Sciences (CAS) under Grant QYZDY-SSW-SMC011, in part by the National Science Foundation of China under Grant 41471363 and Grant 31741016, and in part by the CAS Pioneer Hundred Talents Program. *(Corresponding authors: Yanjun Su; Qinghua Guo.)*

Y. Li is with the State Key Laboratory of Vegetation and Environmental Change, Institute of Botany, Chinese Academy of Sciences, Beijing 100093, China, and also with the University of Chinese Academy of Sciences, Beijing 100049, China (e-mail: ai10056@126.com).

Y. Su and Q. Guo are with the State Key Laboratory of Vegetation and Environmental Change, Institute of Botany, Chinese Academy of Sciences, Beijing 100093, China, and also with the School of Engineering, Sierra Nevada Research Institute, University of California at Merced, Merced, CA 95343 USA (e-mail: suyanjun1987@gmail.com; guo.qinghua@gmail.com).

T. Hu and G. Xu are with the State Key Laboratory of Vegetation and Environmental Change, Institute of Botany, Chinese Academy of Sciences, Beijing 100093, China (e-mail: tianyuhu@ibcas.ac.cn; xuguangcai@ibcas.ac.cn).

Color versions of one or more of the figures in this paper are available online at http://ieeexplore.ieee.org.

Digital Object Identifier 10.1109/TGRS.2018.2843382

I. Introduction

LEAF angle distribution (LAD), as an important canopy structure parameter, has a great influence on the transmission of radiation within vegetation canopy and the distribution of incident photosynthetically active radiation [1]–[3]. It has been considered as a paramount variable in canopy productivity and carbon cycle research of terrestrial ecosystem [4]–[8]. Based on this, LAD is recognized as one of the most important parameters in modeling and understanding biological and physical processes of vegetation, such as photosynthesis, transpiration, radiation transmission, and spectral reflectance [1], [9], [10].

LAD is regarded as one primary factor for the gap fraction model, which is an important and widely used theoretical basis for describing the process of radiative transfer within a vegetative canopy and light interception by a plant canopy [11]. The gap fraction theory was introduced by Monsi and Saeki [12], [13] and developed by Nilson [11] as

$$P(\theta) = \exp[-G(\theta)\Omega L/\cos\theta] \tag{1}$$

where θ is the view zenith angle, $P(\theta)$ represents the probability of a beam or a ray of light penetrating a canopy without being intercepted at an incident angle θ, L denotes the leaf area index, Ω is the clumping index, and $G(\theta)$ is the extinction coefficient defined as the mean projection of a unit foliage area on the plane perpendicular to the view direction θ [3]. The value of $G(\theta)$ can be derived from the LAD function. LAD could be described by the leaf inclination angle and leaf azimuthal angle, which can be defined as the angle between the leaf surface normal and the zenith [3] and the clockwise angle between the north direction and the projection of the principal axis of foliage on the horizontal plane [14], respectively.

Although LAD is so crucial for the balance of mass and energy, few instruments and approaches have been proposed to estimate leaf inclination and azimuthal angles of a single leaf, especially the leaf azimuthal angle. Two major approaches for estimating LAD involve the use of either direct or indirect methods. A simple device consisting of a ruler, magnetic compass, and protractor [15], [16] and a mechanical instrument consisting of high-precision potentiometers with three protruding arms [17] are commonly used to directly measure leaf inclination and azimuthal angles. Direct methods can

produce highly accurate results but have the disadvantages of being extremely laborious and time consuming [18]–[20]. Recently, Ryu *et al.* [21] introduced an indirect method based on digital photography, which has shown the potential to overcome above-mentioned disadvantages of direct methods [22]–[24]. However, this photographic method was carried out based on towers, poles, ladders, unmanned aerial vehicle, and other conventional platform [18] and can only inspect the presence of leaves oriented approximately perpendicular to the viewing direction of the camera [21].

Based on field investigation, different models have been proposed to better characterize LAD, such as the de wit's distribution functions [25], two-parameter Beta-distribution function [4], ellipsoidal distribution function [26], rotated-ellipsoidal distribution function [27], and Verhoef's distribution function [28]. In addition, several approaches have been proposed to compute $G(\theta)$ from the LAD model, such as the Nilson's algorithm [3], [11], [29], Fuchs' algorithm [30], Ross-Goudriaan's algorithm [31], [32], and Suits' algorithm [33]. Note that the above-mentioned models are conducted based on an important assumption that LAD is azimuthally symmetrically distributed (uniform). However, more and more studies have found that this assumption may be often violated in the real world [34]–[36].

Terrestrial laser scanner (TLS), as a ground-based platform, could acquire accurate 3-D information of leaves in high resolution, which provides a new technical means for the accurate retrieval of leaf inclination and azimuthal angles [37], [38]. Many studies have shown that a simple two-parameter Beta-distribution would be the most appropriate for describing LAD of all canopy types [23], [34], [39], [40], and the Beta-distribution holds promise for handling 2-D LAD with two parameters of leaf inclination and azimuthal angles [34].

This paper focused on retrieving the leaf inclination and azimuthal angles using a new method based on leaf point cloud segmentation and filtration, fitting LAD functions based on the two-parameter Beta-distribution model, and finally constructing a projection coefficient model with two parameters using the Nilson's algorithm. To assess the influence of leaf number on leaf inclination and azimuthal angle estimation, we simulated 160 individual leaves and 10 trees with different leaf numbers. In addition, to validate final results, we also sampled three magnolia trees with different leaf numbers and manually measured leaf inclination and azimuthal angles of all their leaves.

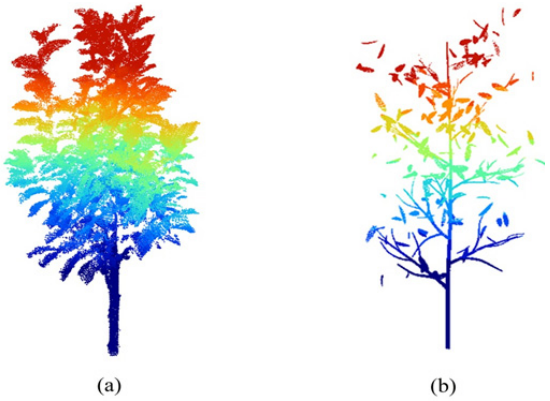

Fig. 1. Samples of point cloud data of individual trees. (a) TLS-based point cloud data. (b) Simulated point cloud data.

TABLE I
SUMMARY OF THE HEIGHT, THE DBH, AND THE NUMBER OF LEAVES FOR 13 TREES. NOTE THAT TREE IDS (1–10) REPRESENT THE SIMULATED TREES AND TREE IDS (11–13) REPRESENT THE SCANNED MAGNOLIA TREES

Tree ID	Tree height (m)	DBH (m)	Leaf size (m × m) (length × width)	No. of leaves
1	2.30	0.05	0.10×0.04	15
2	2.30	0.05	0.10×0.04	30
3	2.30	0.05	0.10×0.04	45
4	2.30	0.05	0.10×0.04	60
5	2.30	0.05	0.10×0.04	75
6	2.30	0.05	0.10×0.04	90
7	2.30	0.05	0.10×0.04	105
8	2.30	0.05	0.10×0.04	120
9	2.30	0.05	0.10×0.04	135
10	2.30	0.05	0.10×0.04	150
11	2.09	0.07	0.10 ×0.08	321
12	3.36	0.10	0.09 ×0.07	617
13	3.60	0.13	0.09 ×0.08	911

Note: The leaf size is the average leaf size per tree.

II. MATERIAL AND METHODS

A. Data Simulation

We modeled 160 individual leaves with different leaf inclination and azimuthal angles for testing the accuracy of the algorithm under the condition that leaves were segmented accurately. At the same time, we simulated 10 trees with different leaf numbers [see Table I: Tree IDs (1–10) and Fig. 1(b)] by means of the stochastic L-system to assess the influence of leaf numbers on the leaf inclination and azimuthal angles estimation. These virtual trees were created in the form of triangle meshes using Weberpenn package [41] in the OpenAlea software. Different virtual trees have the same tree shapes with the same tree height, diameter at breast height (DBH), and the number of branches but different leaf numbers. In this process, the leaf and woody phytoelement (including the trunk, branches, and twigs) could be easily separated. The point cloud data of virtual trees were simulated using the ray-object intersection function of the physically based ray-tracing method [42], which is a general and robust physical rendering system based on the ray tracing algorithm. In this simulation, the virtual trees were "scanned" at azimuth angles of 0°, 90°, 180°, and 270° with a perspective view of 40°, respectively [43], [44]. The true leaf inclination angle information could be easily obtained using the normal vectors

automatically generated during the simulation of the virtual trees. The true leaf azimuthal angles were measured manually using the LiDAR360 (Green Valley International Co., Ltd., China) and Adobe Photoshop software based on the final point cloud data. The principal axis of foliage was determined and marked using a straight line in the LiDAR360 software, and the top view of corresponding leaf point cloud was stored. The true leaf azimuthal angle was obtained by measuring the clockwise angle between the principal axis and x-axis (representing the north direction) using the angle measurement tool of Adobe Photoshop software.

B. Data Collection and Preprocessing

The Riegl VZ-400 TLS (Riegl GmbH, Horn, Austria) mounted on a survey tripod about 1.5 m above the ground was used in this paper to collect point cloud data of three magnolia trees (*Magnolia denudata Desr.*) with different leaf numbers [see Table I: Tree IDs (11–13) and Fig. 1(a)]. We collected the point cloud data for each tree from three different scanning locations during both leaf-on and leaf-off conditions on October 9, 2014, in Beijing, China. The leaf-off TLS scans were conducted after leaf collection. The three different scanning locations for each tree were in a circle with an equal azimuthal angle interval and nearly equal scanning distance. The scanning distance for different trees ranged from 3 to 5 m to guarantee the quality of point cloud data. These scans were performed in a high-speed scanning mode under nearly no-wind conditions. The TLS was set to emit laser beams at fixed steps of 0.04° both vertically and horizontally. To obtain the true ground truth measurements for leaf inclination and azimuthal angles, we measured all leaves of each tree after the leaf-on TLS scans using the device proposed by Norman and Campbell [15]. The device is consisted of a ruler, magnetic compass, and protractor. We measured the leaf inclination angle by controlling the top of the instrument to be parallel to the leaf plane. At the same time, the direction of instrument placement should be consistent with leaf expansion direction. The leaf azimuthal angle was measured by measuring the clockwise angle between the north direction and the leaf expansion direction. The errors for the device may be caused by inaccurate placement of instrument, and the change of leaf position by wind may be another error source. Therefore, each leaf was measured three times under no-wind conditions, and the mean value of the three measurements was adopted to ensure the accuracy of validation data in this paper.

The effects of outliers, occlusion, and woody phytoelement points are the three important factors influencing the quality of the point cloud data. In this paper, we removed outliers using the statistical outlier removal filter in the point cloud library. Two parameters of this statistical filter, the number of neighboring points n and the multiplier of the standard deviation (STD) k, were set at 30 and 1, respectively. The iterative closest point algorithm [45] integrated into the RiSCAN PRO software was used to register multilocation scanning data. The root-mean-square errors (RMSE) for the registration process were smaller than 0. 002 m. Finally, the woody phytoelement points of each tree were removed using a range search method based on leaf-on and leaf-off point clouds of the same tree [46]. As to the simulated point cloud data, we do not need the above-mentioned denoising and registration process. As to the simulated point cloud data, we do not need the above-mentioned denoising and registration process, since the simulated point cloud data have no outliers and the data from four different "scanning" positions have the same coordinate system. In addition, the woody-leaf phytoelement separation could be automatically finished in the process of virtual tree creation. Therefore, we could obtain high-quality simulated leaf point cloud data after woody-leaf phytoelement separation and data merging.

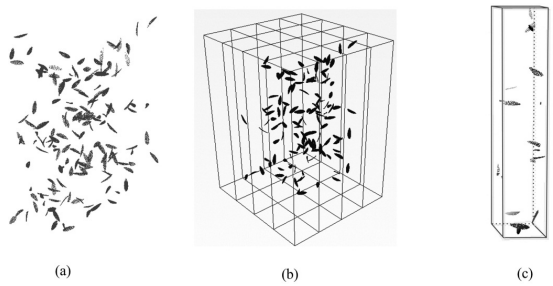

Fig. 2. Illustration for point cloud voxelization. (a) Leaf point cloud data. (b) Voxelization. and (c) Leaf point cloud data for a single voxel.

C. Leaf Inclination and Azimuthal Angles Estimation

1) Voxelization: After the data preprocessing, leaf point cloud data of each tree was first translated by transforming the central point of each leaf point cloud data into the origin point of the Cartesian coordinate system. Then, we voxelized the leaf points using the voxel-based canopy profiling method [47]. The width and length of a voxel were defined as twice of the maximum leaf length of each tree, and the height of a voxel was determined by the difference between the minimum and maximum values of z-coordinates (see Fig. 2). The leaf point cloud data were divided into a finite number of small parts through voxelization, and each voxel was regarded as the basic computing unit.

2) Leaf Segmentation and Filtration: Accurate leaf segmentation is an important prerequisite for the retrieval of leaf inclination and azimuthal angles. After voxelization, we adopted a cluster algorithm proposed by Ester *et al.* [48] named density-based spatial clustering of applications with noise (DBSCAN) for leaf segmentation. DBSCAN is little influenced by outliers and does not require to specify the number of clusters as an input parameter [48], [49]. Two parameters are required by DBSCAN: the minimum number of points (MinPts) required to form a cluster and the maximum radius of the neighborhood from the core point (Eps). This algorithm starts with an arbitrary point that has not been visited and its neighborhood points within a distance of Eps are retrieved. If the number of neighborhood points (including this point itself) is greater than MinPts, a cluster is initiated; otherwise, the point is labeled as noise. This process is repeated until every point has been visited. The MinPts is set at 30 in this paper, which is closely related to the point cloud density. The Eps could be calculated from the MinPts and the

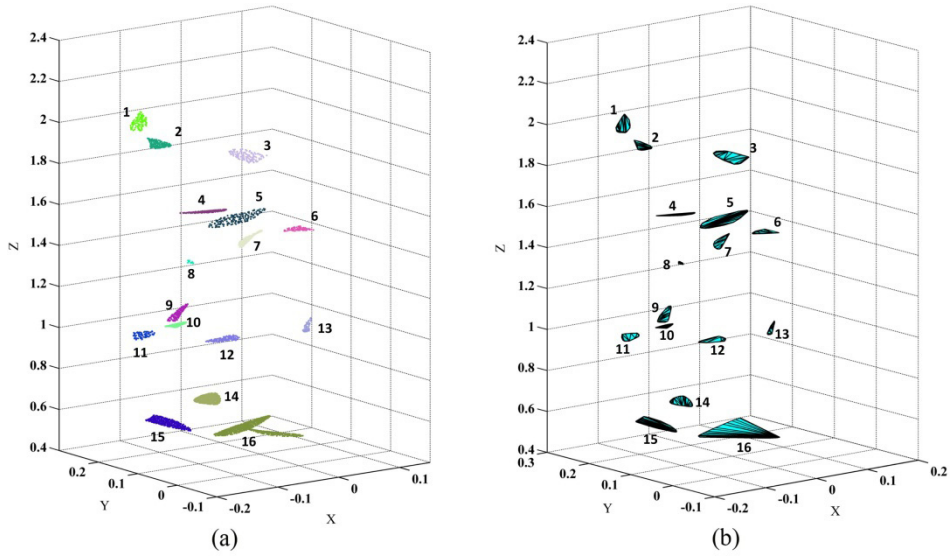

Fig. 3. Leaf point cloud clustering analysis and 3-D convex hull construction. (a) Final clustering results. (b) 3-D convex hull for each cluster. The numbers 1–16 represent the different clusters.

size of the point cloud using the following equations [50]:

$$Eps = \sqrt{\frac{T \cdot MinPts \cdot \Gamma[(1/2) \cdot n + 1]}{m\sqrt{\pi^n}}}$$
$$T = \prod_{i=1}^{n} \{\max(X_i) - \min(X_i)\} \tag{2}$$

where n denotes the dimensionality of points, m is the number of points, X is the point data set, and T is the volume of the experimental space formed by m points.

After the clustering analysis using the DBSCAN algorithm, leaf points in the same voxel were segmented into different clusters [from Figs. 2(c)–3(a)]. We constructed 3-D convex hull for each cluster [see Fig. 3(b)], and one-half of the total surface area of the 3-D convex hull was regarded as the surface area of a cluster in reality [19]. The cluster, whose one-half of surface area is greater than 2/3 of the manually measured single leaf area and smaller than manually measured single leaf area (leaves 4, 5, 14, and 15 in Fig. 3), was selected as the point cloud data of a complete leaf and removed from the raw point cloud data. The true leaf area was collected by manual measurements. The clusters with incomplete leaves (leaves 1–3 and 6–13 in Fig. 3) and several leaves (leaf 16 in in Fig. 3) were retained. In addition, to get more point cloud data of complete leaves, we voxelized the rest of leaf point clouds and repeated the above-mentioned process after data rotation until no more complete leaf could be found. The rotation was performed around the z-axis from 30° to 360° with an interval 30°. The leaf recognition ratio and correction ratio after leaf segmentation and filtration were then calculated. The leaf recognition ratio is the ratio of the number of segmented leaves and total number of leave for each tree. The correction ratio is the ratio of the number of corrected segmented leaves and the total number of segmented leaves. Visual inspection was adopted to judge whether the segmentation was correct or not.

3) Leaf Inclination and Azimuthal Angle Estimation: After leaf segmentation and filtration, we constructed the covariance matrix for each complete leaf point cloud data using (3) to retrieve leaf inclination and azimuthal angles

$$M = \begin{pmatrix} \mathrm{cov}(x,x) & \mathrm{cov}(x,y) & \mathrm{cov}(x,z) \\ \mathrm{cov}(y,x) & \mathrm{cov}(y,y) & \mathrm{cov}(y,z) \\ \mathrm{cov}(z,x) & \mathrm{cov}(z,y) & \mathrm{cov}(z,z) \end{pmatrix}$$
$$o_i = (1/n)\sum_{i=1}^{n} p_i$$
$$\mathrm{cov}(i,j) = \frac{\sum_1^n (p_i - o_i)(p_j - o_j)^{\mathrm{T}}}{n-1} \tag{3}$$

where M is the covariance matrix, (x, y, z) are the three variables and corresponding to first, second, and third column of point cloud data, o_i is the average value of all elements of the ith column, p_i and p_j are all elements of the ith and jth column, respectively, and n is the number of points. The eigenvectors (e_1, e_2, and e_3) and the corresponding eigenvalues (λ_1, λ_2, and λ_3) of the covariance matrix are extracted. Assuming that $\lambda_1 > \lambda_2 > \lambda_3$, the eigenvector e_3 would be considered as the normal vector of a leaf plane. The leaf inclination angle was calculated as the angle between the eigenvector e_3 and the vector (0, 0, 1). The eigenvector e_1 represents the direction of leaf principal axis under the assumption that the leaf length was greater than the leaf width, and leaf azimuthal angle was calculated as the angle between the eigenvector e_1 and the vector representing the north direction. Note that the direction of the eigenvector e_1 describing as (a, b, c) could be either upward or downward, which means that the value of e_1 has two possibilities: (a, b, c) or $(-a, -b, -c)$. In this paper, we assumed that the direction of leaf principal axis is downward, and the eigenvector e_1 would be reversed by multiplying by -1 under the condition that the value of c is greater than zero. In addition, we rotated the leaf data to obtain more complete leaf point cloud data in Section II-C2.

Therefore, we should subtract the corresponding angle of rotation to obtain true leaf azimuthal angle.

D. LAD and G-Function Construction

The two-parameter Beta-distribution has been found to be the best for describing the probability density of leaf inclination angle [39] and have the potential to handle the probability density of leaf azimuthal angle [34]. Therefore, after leaf inclination and azimuthal angle estimation, we fit the measured leaf inclination and azimuthal angle with the two-parameter Beta-distribution [4], [40] in (4)–(7), which is based on an important assumption that the distribution of leaf inclination angle is independent of leaf azimuthal angle distribution

$$f(t) = \frac{1}{B(\mu+\nu)}(1-t)^{\mu-1}t^{\nu-1} \tag{4}$$

where $t = 2\theta_L/\pi$. The Beta-distribution function $B(\mu, \nu)$ is defined as

$$B(\mu,\nu) = \int_0^1 (1-x)^{\mu-1}x^{\nu-1}dx = \frac{\Gamma(\mu)\Gamma(\nu)}{\Gamma(\mu+\nu)} \tag{5}$$

where Γ is the Gamma function, μ and ν are the two parameters that can be calculated as

$$\mu = (1-\overline{t})\left(\frac{\sigma_0^2}{\sigma_t^2}-1\right) \tag{6}$$

$$\nu = \overline{t}\left(\frac{\sigma_0^2}{\sigma_t^2}-1\right) \tag{7}$$

where σ_0^2 is the maximum STD with expected mean $\overline{t}$ ($\sigma_0^2 = \overline{t}(1-\overline{t})$) and σ_t^2 is the variance of t [39]. After fitting LAD using two-parameter Beta-distribution function, we can write the extinction coefficient function $G(\theta, \varphi)$ as follows:

$$G(\theta,\varphi) = \int_0^{\pi/2}\int_0^{2\pi} A(\theta,\theta_L,\varphi,\varphi_L)f(\theta_L)f(\varphi_L)d\varphi_L d\theta_L \tag{8}$$

where A is the projection coefficient for the leaf inclination angle θ, the leaf azimuth angle φ, the view zenith angle θ_L, and the view azimuthal angle φ_L [29]

$$A(\theta,\theta_L,\varphi,\varphi_L) = |\cos\theta\sin\theta_L - \sin\theta\cos\theta_L(\cos(\varphi-\varphi_L))|. \tag{9}$$

III. RESULTS

A. Leaf Inclination and Azimuthal Angles Estimation Based on Simulated Point Cloud Data

Leaf inclination and azimuthal angles were retrieved based on simulated point cloud data of individual leaves. Fig. 4 shows the scatter plots between the leaf inclination and azimuthal angles of individual leaves estimations and manually measured values. The leaf inclination and azimuthal angle estimations were in a good agreement with values obtained from actual measurements ($R^2 = 0.98$, RMSE = 2.41° and $R^2 = 0.99$, RMSE = 3.44°, respectively; Fig. 4). The estimation of leaf inclination angle was achieved with smaller absolute error comparing to leaf azimuthal angle estimation (2.41° versus 3.44° in RMSE), while leaf azimuthal angle estimation achieved smaller relative error. Note that this accuracy assessment for leaf inclination and azimuthal angles was only performed for the simulated data, because it was difficult for leaves to achieve consistent one-to-one match between TLS-based data and actual measurements.

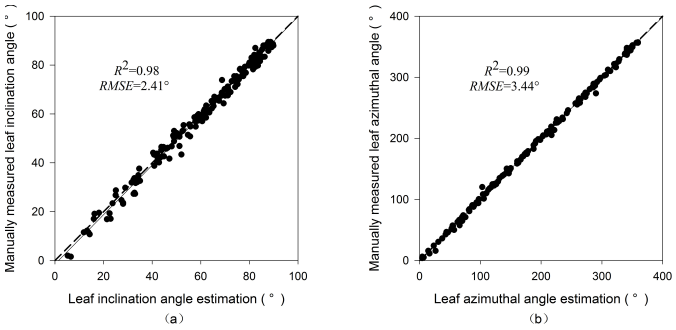

Fig. 4. Scatter plots showing the relationship between the leaf inclination and azimuthal angle estimations from simulated data and ground truth measurements. (a) Leaf inclination angle estimation. (b) Leaf azimuthal angle estimation. Dashed line: 1:1 relationship. Solid line: fit line.

TABLE II
TOTAL LEAF NUMBER, NUMBER OF SEGMENTED LEAVES, NUMBER OF TRUE SEGMENTED LEAVES, AND CORRESPONDING RECOGNITION RATIO AND CORRECTION RATIO FOR EACH TREE. NOTE THAT TREE IDS (1–10) REPRESENT SIMULATED TREES AND TREE IDS (11–13) REPRESENT SCANNED MAGNOLIA TREES

Tree ID	No. of leaves	No. of segmented leaves	No. of true segmented leaves	Recognition ratio (%)	Correction ratio (%)
1	15	15	15	100	100
2	30	28	28	93	100
3	45	43	43	95	100
4	60	54	54	90	100
5	75	67	67	89	100
6	90	82	82	91	100
7	105	94	94	89	100
8	120	102	102	85	100
9	135	117	117	86	100
10	150	120	120	80	100
11	321	102	35	32	34
12	617	172	37	28	22
13	911	212	28	23	13

B. Leaf Segmentation and LAD Fitting Based on Simulated and Measured Point Cloud Data

We modeled 10 trees and scanned 3 magnolia trees with different leaf numbers (Table I) to further assess the influence of leaf numbers on the accuracy of leaf segmentation and LAD fitting. Results showed that for the simulated trees, the leaf

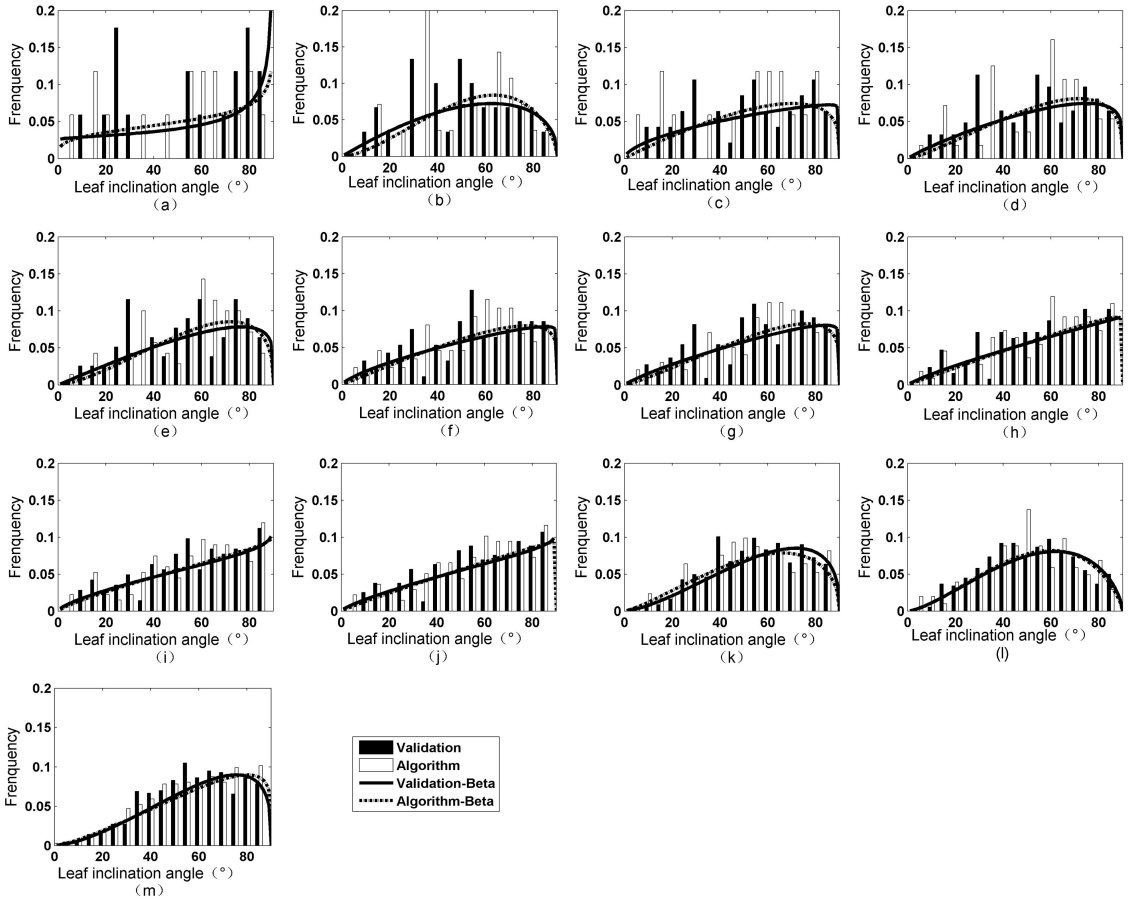

Fig. 5. Histogram and fit Beta-distributions of leaf inclination angle for trees with different leaf numbers. (a)–(j) Different simulated trees. (k)–(m) Different TLS-based trees.

recognition ratio decreased with the increase of leaf numbers, but the leaf correction ratio with high value had no change [Table II: Tree IDs (1–10)]; whereas for the TLS-based magnolia trees, the leaf recognition ratio and the leaf correction ratio decreased with the increase of leaf numbers [Table II: Tree IDs (11–13)].

Based on leaf segmentation, we calculated the leaf inclination and azimuthal angles for each segmented leaf and fit LAD using the two-parameter Beta function. Figs. 5 and 6 show the comparison of leaf inclination and azimuthal angle estimations with true values for these 13 trees (10 simulated trees and 3 TLS-based magnolia trees), respectively. The bin width of LAD histogram in Figs. 5 and 6 was set at 5°. By observing the leaf inclination angle distribution pattern of different trees (see Fig. 5), it can be found that the pattern of distribution has a relatively significant variation from Fig. 5(a)–(e) and the distribution pattern has no significant changes from Fig. 5(f)–(j) for the simulated trees. In addition, the leaf inclination angle distribution pattern of TLS-based trees has few changes [see Fig. 5(k)–(m)]. Moreover, there was a little difference among the leaf azimuthal angle distribution pattern of different trees (see Fig. 6).

Our results strongly supported that the LAD algorithm proposed in this paper can deliver equivalent leaf inclination (see Fig. 5) and azimuthal (see Fig. 6) angle distribution results to the distributions generated from ground truth data for both simulated and TLS-based trees. The mean leaf inclination and azimuthal angle distributions for each tree has no significant difference with validation values (t-test, $p > 0.05$). The more rigorous two-sample Kolmogorov–Smirnov (K–S) test [51] for homogeneity of the leaf inclination and azimuthal angle distributions from the algorithm and validation values was also accepted at $p > 0.05$ significance level for both simulated and TLS-based trees (Figs. 5 and 6), expect the leaf azimuthal angle distribution of trees 2, 3, and 4 [$0.04 < p < 0.05$, Fig. 6(b)–(d)].

C. Projection Coefficient Model With Two Parameters Construction

On the basis of accurately extracted leaf inclination and azimuthal angles, we constructed the projection coefficient model $G(\theta, \varphi)$ with two parameters for both simulated data and TLS-based point cloud data. Results showed that the projection coefficient models based on algorithm were in relatively good agreements with those models obtained from validation values for different trees with different leaf numbers (K–S test, $p > 0.05$). The change of difference between coefficient models based on algorithm and those models obtained from validation values showed that the degree of agreement

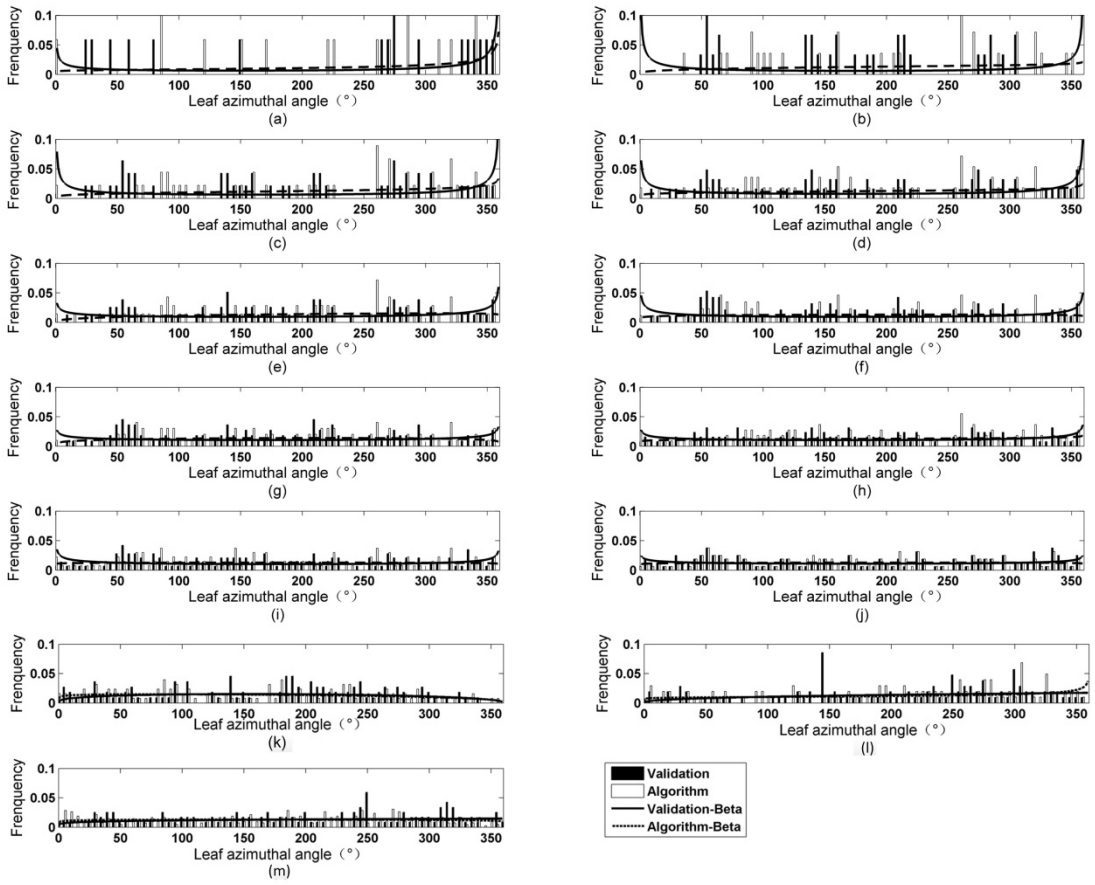

Fig. 6. Histogram and fit Beta-distributions of leaf azimuthal angle for trees with different leaf numbers. (a)–(j) Different simulated trees. (k)–(m) Different TLS-based trees.

increased with the leaf numbers (see Fig. 7). In addition, the $G(\theta, \varphi)$ value decreased with the increase of view zenith angle but stayed relatively stable with the varying view azimuthal angles.

IV. Discussion

In our results, the leaf azimuthal angles were retrieved with larger absolute error than leaf inclination angles in the individual leaf level (see Fig. 4). This phenomenon can be explained by the assumption that the leaf azimuthal angles were extracted under the condition that the leaf length was greater than the leaf width. The leaf asymmetries and the incompleteness of leaf point cloud data would not be likely to support the above-mentioned assumption and finally decreased leaf azimuthal angle estimation precision. In addition, leaf azimuthal angle retrieval in this paper is based on another important assumption that the direction of leaf principal axis was downward. In fact, the direction of leaf principal axis under the natural condition could be either upward or downward, which would result in uncertainty of leaf azimuthal angle retrieval. The smaller relative error of leaf azimuthal angle estimation was determined by its large value range (0°–360°). Note that the leaf inclination and azimuthal angle retrieval algorithm in this paper was applicable for deciduous forests and may not be directly transferred to coniferous forest.

In the voxel-based leaf segmentation method, voxelization and rotation were conducted to achieve accurate retrieval of leaf inclination and azimuthal angles at the individual tree level. The voxel size and rotation interval could be modified properly according to the actual condition of point cloud data. Results showed that the leaf recognition ratio decreased for both simulated and TLS-based data as the leaf numbers increased (see Table II). This phenomenon could be explained by that the degree of aggregation in leaf distribution increased as the leaf numbers increased, and high leaf aggregation degree would greatly increase the difficulty of leaf segmentation and decrease the leaf recognition ratio. Besides the number of leaves, tree sizes (e.g., tree height and DBH) may also influence the leaf recognition accuracy by interacting with the number of leaves. Therefore, we analyzed the influence of different factors on the leaf recognition accuracy (see Fig. 8). Result shows that although tree height and DBH have influence on the leaf recognition ratio, their influence is much smaller than the number of leaves and the scanning resolution. Multilocation scanning and short scanning distance were adopted in this paper to guarantee the scanning resolution. How the interaction between tree sizes and the number of leaves influence the leaf recognition accuracy still needs to be further studied. Comparing to the simulated data, the leaf recognition rate and recognition correction rate of the TLS-based point cloud data were generally lower (see Table II). Besides leaf numbers,

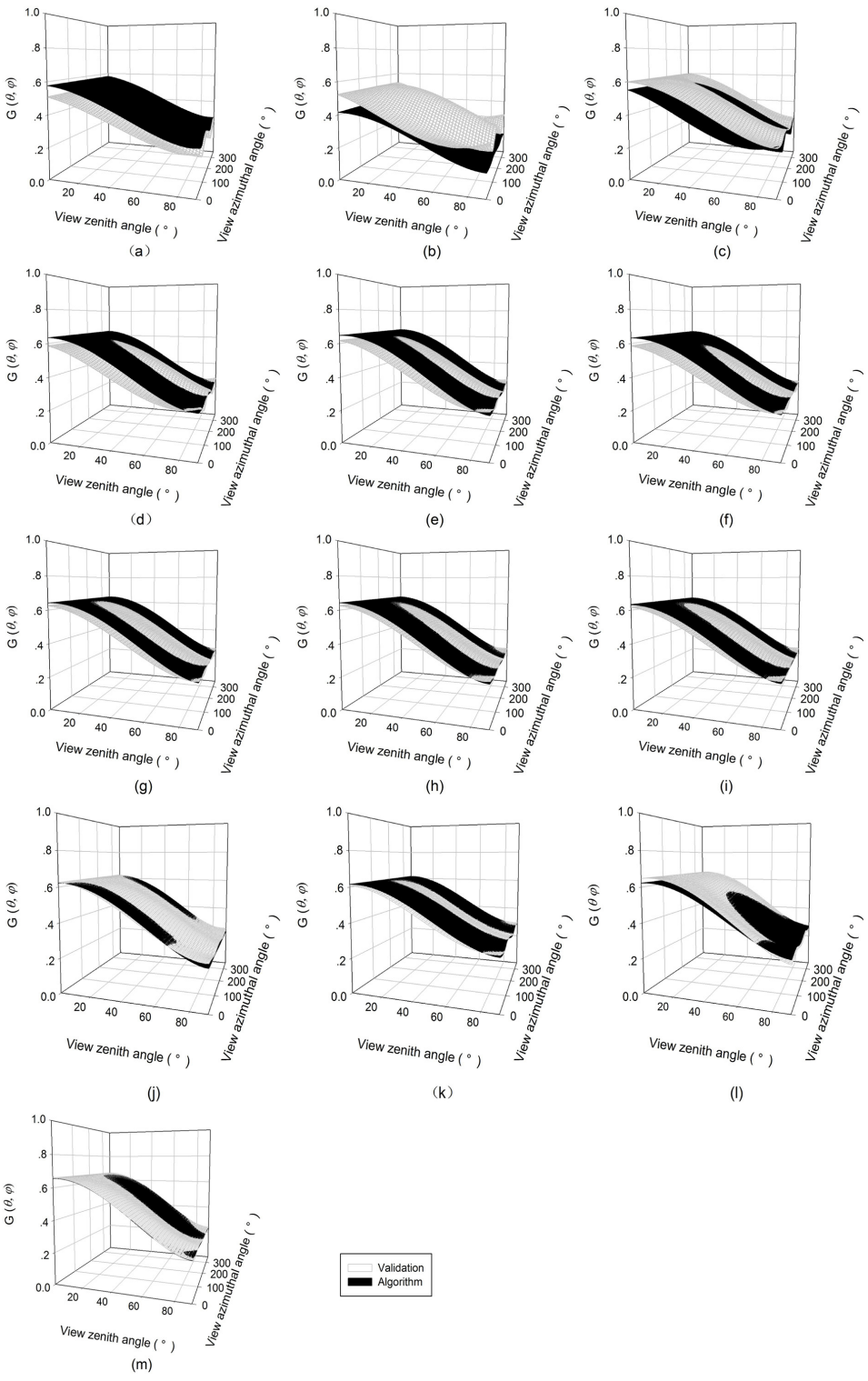

Fig. 7. Projection coefficient model $G(\theta, \varphi)$ of 13 trees against view zenith angle θ_L and the view azimuth angle φ_L based on two data sets generated from algorithm and validation values, respectively. (a)–(j) Different simulated trees. (k)–(m) Different TLS-based trees.

the quality of the point cloud data (including accuracy and completeness) was another important factor that gave rise to the above-mentioned phenomenon. The low leaf recognition correction rate for the TLS-based data was primarily caused by the incompleteness of the segmented leaves. Differing from simulated data, the quality of TLS-based data was affected by three factors: outliers, woody phytoelement points, and occlusion. Although we have removed the outliers and the woody phytoelement points, and performed registration in the RiSCAN PRO software with high accuracy, the influence of these three factors could not be totally eliminated. The quality of TLS-based data still had space to improve. Therefore, how

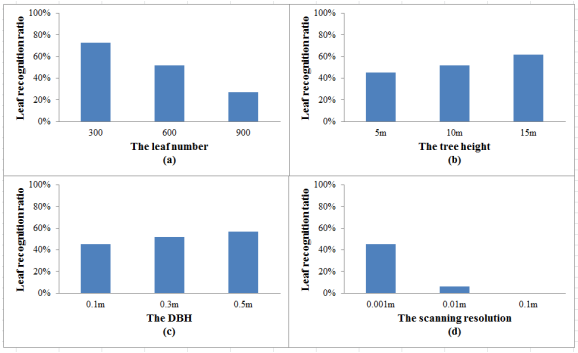

Fig. 8. Influence of different factors on the leaf recognition ratio. (a) Leaf number. (b) Tree height. (c) DBH. (d) Scanning resolution.

to better achieve denoising, separation of woody points from foliage points, and registration for TLS-based data would be a great challenge to accurate leaf segmentation in the future studies.

Results showed that LAD could be retrieved accurately based on leaf segmentation for different trees with different leaf numbers (see Figs. 5 and 6). The bin width of LAD histogram was determined by the estimation accuracy of leaf inclination and azimuthal angles in the individual leaf level (see Fig. 4). The accuracy of LAD estimations was little affected by the low leaf recognition and recognition correction rates for trees with a large number of leaves [see Figs. 5(k)–(m) and 6(k)–(m)], and the LAD pattern tended to be consistent as leaf number increased (see Figs. 5 and 6). This result agreed with previous reports that reliable estimation of LAD can be obtained by measuring the leaf angles of approximately 75 leaves [23]. This might also explain why the accuracy of LAD estimation was kept well under such low leaf recognition and recognition correction rate condition for TLS-based data [see Figs. 5(k)–(m) and 6(k)–(m)]. Therefore, comparing to the previous study that the whole point cloud data of a tree involved in the estimation of LAD [19], [38], we calculated the LAD based on a certain number of segmented complete leaves. This method could guarantee LAD estimation accuracy under the condition that the accuracy and completeness of TLS-based point cloud data still have room for improvement after data preprocessing (including denoising, removing the woody phytoelement points, and registration). In addition, the filtration was conducted after leaf segmentation, and the filter criteria was greater than 2/3 of the manually measured single leaf area and smaller than the manually measured single leaf area. This filter criteria could filter the individual leaf from several clusters and guarantee the completeness of the segmented leaf to some extent.

The change characteristics of $G(\theta, \varphi)$ showed in Fig. 7 was determined by the pattern of LAD of simulated and TLS-based data (see Figs. 5 and 6). Note that the construction of $G(\theta, \varphi)$ was based on an important assumption that leaf inclination and azimuthal angles were statistically independent in this paper. A new equation differing from (8) should be proposed under the condition that they have strongly correlation. Comparing to the traditional one-parameter projection coefficient model $G(\theta)$ [3], [4], [11], [26], two parameters $G(\theta, \varphi)$ proposed in this paper combined the leaf inclination and azimuthal angle distribution well, which was important for accurate models of vegetation canopy reflectance. Meanwhile, two parameters $G(\theta, \varphi)$ appeared to be a versatile tool for the research of the light distribution within canopy.

All results showed that the new method based on point cloud data proposed in this paper can provide LAD and $G(\theta, \varphi)$ estimations with high accuracy (see Figs. 4–7). Unlike what was commonly assumed in previous studies that the LAD was azimuthally symmetric due to the restriction of measurement techniques [11], [26], [33], [39], a new point cloud-based algorithm was proposed for accurate extraction of leaf azimuthal angle in this paper. Based on this, two-parameter projection coefficient model was constructed, which provides a new perspective with respect to 2-D LAD and projection coefficient model retrieval. In addition, this point cloud-based method could overcome the problem of the traditional measurements that were extremely time-consuming and labor intensive [18], [19], [20].

V. Conclusion

In this paper, the leaf inclination and azimuthal angles as well as LAD were retrieved, and the projection coefficient model with two parameters $G(\theta, \varphi)$ was constructed using a new algorithm based on point cloud data generated from simulated and TLS-based data. By comparing TLS measurements with those obtained from actual measurement, this paper demonstrated that TLS data can provide statistically similar LAD and $G(\theta, \varphi)$ estimations. It was found that leaf number is a factor influencing more leaf recognition and recognition correction ratio than LAD and $G(\theta, \varphi)$ estimations in this paper. Note that the high quality of the point cloud data was a major basis of accurate LAD and $G(\theta, \varphi)$ estimations. The theories and methods used in this paper may also be applicable to a forest at the stand level under the prerequisite of guaranteeing the quality of TLS-based point cloud data.

References

[1] G. P. Asner, "Biophysical and biochemical sources of variability in canopy reflectance," *Remote Sens. Environ.*, vol. 64, no. 3, pp. 234–253, Jun. 1998.

[2] R. Houborg, H. Soegaard, and E. Boegh, "Combining vegetation index and model inversion methods for the extraction of key vegetation biophysical parameters using Terra and Aqua MODIS reflectance data," *Remote Sens. Environ.*, vol. 106, pp. 39–58, Jan. 2007.

[3] J. Ross, *The Radiation Regime and Architecture of Plant Stands* (Tasks for Vegetation Science), vol. 3, H. Lieth, Ed. New York, NY, USA: Springer, 1981.

[4] N. S. Goel and D. E. Strebel, "Simple beta distribution representation of leaf orientation in vegetation canopies," *Agronomy J.*, vol. 76, no. 5, pp. 800–802, 1984.

[5] V. P. Gutschick, "Joining leaf photosynthesis models and canopy photon-transport models," in *Photon-Vegetation Interaction*, R. G. Myneni and J. Ross, Eds. Berlin, Germany: Springer-Verlag, 1991, pp. 501–535.

[6] Ü. Niinemets, "A review of light interception in plant stands from leaf to canopy in different plant functional types and in species with varying shade tolerance," *Ecol. Res.*, vol. 25, no. 4, pp. 693–714, Jul. 2010.

[7] C. J. Kucharik, J. M. Norman, and S. T. Gower, "Measurements of leaf orientation, light distribution and sunlit leaf area in a boreal aspen forest," *Agricult. Forest Meteorol.*, vol. 91, pp. 127–148, May 1998.

[8] K. Zhao, S. Popescu, and R. Nelson, "LiDAR remote sensing of forest biomass: A scale-invariant estimation approach using airborne lasers," *Remote Sens. Environ.*, vol. 113, no. 1, pp. 182–196, 2009.

[9] J. W. Wilson, "Analysis of the spatial distribution of foliage by two-dimensional point quadrats," *New Phytol.*, vol. 58, no. 1, pp. 92–99, 1959.

[10] R. B. Myneni, "A review on the theory of photon transport in leaf canopies," *Agricult. Forest Meteorol.*, vol. 45, pp. 1–153, Feb. 1989.

[11] T. Nilson, "A theoretical analysis of the frequency of gaps in plant stands," *Agricult. Meteorol.*, vol. 8, pp. 25–38, Jan. 1971.

[12] M. Monsi and T. Saeki, "Uber den lichtfaktor in den pflanzengesellschaften und seine bedeutung fur die stoffproduktion," *Jpn. J. Botany*, vol. 14, no. 1, pp. 22–52, 1953.

[13] M. Monsi and T. Saeki, "On the factor light in plant communities and its importance for matter production," *Ann. Botany*, vol. 95, no. 3, pp. 549–567, 2005.

[14] D. G. Lugg, V. E. Youngman, and G. Hinze, "Leaf azimuthal orientation of sorghum in four row directions," *Agronomy J.*, vol. 73, no. 3, pp. 497–500, 1981.

[15] J. M. Norman and G. S. Campbell, "Canopy structure," in *Plant Physiological Ecology: Field Methods Instrumentation*, R. W. Pearcy *et al.*, Eds. New York, NY, USA: Chapman & Hall, 1989, pp. 301–325.

[16] G. S. Campbell and J. M. Norman, *An Introduction to Environmental Biophysics*, 2nd ed. New York, NY, USA: Springer, 1998.

[17] A. R. G. Lang, "Leaf orientation of a cotton plant," *Agricult. Meteorol.*, vol. 11, pp. 37–51, Jan. 1973.

[18] C. S. T. Daughtry, "Direct measurements of canopy structure," *Remote Sens. Rev.*, vol. 5, no. 1, pp. 45–60, 1990.

[19] G. Zheng and L. M. Moskal, "Computational-geometry-based retrieval of effective leaf area index using terrestrial laser scanning," *IEEE Trans. Geosci. Remote Sens.*, vol. 50, no. 10, pp. 3958–3969, Oct. 2012.

[20] X. Zou and M. Mõttus, "Retrieving crop leaf tilt angle from imaging spectroscopy data," *Agricult. Forest Meteorol.*, vol. 205, pp. 73–82, Jun. 2015.

[21] Y. Ryu *et al.*, "How to quantify tree leaf area index in an open savanna ecosystem: A multi-instrument and multi-model approach," *Agricult. Forest Meteorol.*, vol. 150, pp. 63–76, Jan. 2010.

[22] J. Pisek, Y. Ryu, and K. Alikas, "Estimating leaf inclination and G-function from leveled digital camera photography in broadleaf canopies," *Trees*, vol. 25, pp. 919–924, Oct. 2011.

[23] J. Pisek, O. Sonnentag, A. D. Richardson, and M. Mõttus, "Is the spherical leaf inclination angle distribution a valid assumption for temperate and boreal broadleaf tree species?" *Agricult. Forest Meteorol.*, vol. 169, pp. 186–194, Feb. 2013.

[24] X. Zou *et al.*, "Photographic measurement of leaf angles in field crops," *Agricult. Forest Meteorol.*, vol. 184, pp. 137–146, Jan. 2014.

[25] C. T. de Wit, "Photosynthesis of leaf canopies," Center Agricult. Publication Documents, Wageningen Univ. Res., Wageningen, The Netherlands, Tech. Rep. 663, 1965.

[26] G. S. Campbell, "Derivation of an angle density function for canopies with ellipsoidal leaf angle distributions," *Agricult. Forest Meteorol.*, vol. 49, pp. 173–176, Feb. 1990.

[27] S. C. Thomas and W. E. Winner, "A rotated ellipsoidal angle density function improves estimation of foliage inclination distributions in forest canopies," *Agricult. Forest Meteorol.*, vol. 100, pp. 19–24, Jan. 2000.

[28] W. Verhoef, "Theory of radiative transfer models applied in optical remote sensing of vegetation canopies," Ph.D. dissertation, Wageningen Univ. Res., Wageningen, The Netherlands, 1997.

[29] J. W. Wilson, "Incliend point quadrats," *New Phytol.*, vol. 59, pp. 1–7, Apr. 1960.

[30] M. Fuchs, G. Asrar, E. T. Kanemasu, and L. E. Hipps, "Leaf area estimates from measurements of photosynthetically active radiation in wheat canopies," *Agricult. Forest Meteorol.*, vol. 32, no. 1, pp. 13–22, 1984.

[31] J. Ross, "Radiative transfer in plant communities," in *Vegetation and the Atmosphere*. New York, NY, USA: Academic, 1975, pp. 13–55.

[32] J. Goudriaan, "Crop micrometeorology: A simulation study," Center Agricult. Publishing Documents, Wageningen Univ. Res., Wageningen, The Netherlands, Tech. Rep. 249, 1977.

[33] G. H. Suits, "The calculation of the directional reflectance of a vegetative canopy," *Remote Sens. Environ.*, vol. 2, pp. 117–125, Jan. 1971.

[34] D. E. Strebel, N. S. Goel, and K. J. Ranson, "Two-dimensional leaf orientation distributions," *IEEE Trans. Geosci. Remote Sens.*, vol. GRS-23, no. 5, pp. 640–647, Sep. 1985.

[35] D. S. Kimes and J. A. Kirchner, "Diurnal variations of vegetation canopy structure," *Int. J. Remote Sens.*, vol. 4, no. 2, pp. 257–271, 1983.

[36] L. Ma, G. Zheng, J. U. H. Eitel, T. S. Magney, and L. M. Moskal, "Retrieving forest canopy extinction coefficient from terrestrial and airborne LiDAR," *Agricult. Forest Meteorol.*, vol. 15, pp. 1–21, Apr. 2017.

[37] F. Hosoi, Y. Nakai, and K. Omasa, "Estimating the leaf inclination angle distribution of the wheat canopy using a portable scanning LiDAR," *J. Agricult. Meteorol.*, vol. 65, no. 3, pp. 297–302, 2009.

[38] G. Zheng and L. M. Moskal, "Leaf orientation retrieval from Terrestrial Laser Scanning (TLS) data," *IEEE Trans. Geosci. Remote Sens.*, vol. 50, no. 10, pp. 3970–3979, Oct. 2012.

[39] W.-M. Wang, Z.-L. Li, and H.-B. Su, "Comparison of leaf angle distribution functions: Effects on extinction coefficient and fraction of sunlit foliage," *Agricult. Forest Meteorol.*, vol. 143, pp. 106–122, Mar. 2007.

[40] B. E. McNeil, J. Pisek, H. Lepisk, and E. A. Flamenco, "Measuring leaf angle distribution in broadleaf canopies using UAVs," *Agricult. Forest Meteorol.*, vols. 218–219, pp. 204–208, Mar. 2016.

[41] J. Weber and J. Penn, "Creation and rendering of realistic trees," in *Proc. 22nd Annu. Conf. Comput. Graph. Interact. Techn.*, 1995, pp. 119–128.

[42] M. Pharr and G. Humphreys, *Physically Based Rendering: From Theory to Implementation*. Burlington, MA, USA: Morgan Kaufmann, 2004.

[43] J.-F. Côté, J.-L. Widlowski, R. A. Fournier, and M. M. Verstraete, "The structural and radiative consistency of three-dimensional tree reconstructions from terrestrial LiDAR," *Remote Sens. Environ.*, vol. 113, no. 5, pp. 1067–1081, 2009.

[44] S. Tao, Q. Guo, S. Xu, Y. Su, Y. Li, and F. Wu, "A geometric method for wood-leaf separation using terrestrial and simulated LiDAR data," *Photogramm. Eng. Remote Sens.*, vol. 81, pp. 767–776, Oct. 2015.

[45] P. J. Besl and N. D. McKay, "A method for registration of 3-D shapes," *IEEE Trans. Pattern Anal. Mach. Intell.*, vol. 14, no. 2, pp. 239–256, Feb. 1992.

[46] Y. Li *et al.*, "Derivation, validation, and sensitivity analysis of terrestrial laser scanning-based leaf area index," *Can. J. Remote Sens.*, vol. 42, no. 6, pp. 719–729, 2016.

[47] F. Hosoi and K. Omasa, "Voxel-based 3-D modeling of individual trees for estimating leaf area density using high-resolution portable scanning LiDAR," *IEEE Trans. Geosci. Remote Sens.*, vol. 44, no. 12, pp. 3610–3618, Dec. 2006.

[48] M. Ester, H. P. Kriegel, J. Sander, and X. Xu, "A density-based algorithm for discovering clusters in large spatial databases with noise," in *Proc. KDD*, vol. 96, Aug. 1996, pp. 226–231.

[49] J. Wu, K. Cawse-Nicholson, and J. van Aardt, "3D Tree reconstruction from simulated small footprint waveform LiDAR," *Photogramm. Eng. Remote Sens.*, vol. 79, pp. 1147–1157, Dec. 2013.

[50] M. Daszykowski, B. Walczak, and D. L. Massart, "Looking for natural patterns in analytical data. 2. Tracing local density with OPTICS," *J. Chem. Inf. Comput. Sci.*, vol. 42, no. 3, pp. 500–507, May/Jun. 2002.

[51] R. R. Sokal and J. F. Rohlf, *Biometry: The Principles and Practice of Statistics in Biological Research*, 2nd ed. San Francisco, CA, USA: Freeman, 1981.

Yumei Li received the B.S. degree in ecology from Hebei Agricultural University, Hebei, China, in 2012, and the Ph.D. degree from the Institute of Botany, Chinese Academy of Sciences, Beijing, China, in 2018.

Her current research interests include the studies on retrieval method of structural and biophysical parameters of vegetation using light detection and ranging (LiDAR) data and using remote sensing technology to answer key scientific issues on ecological science.

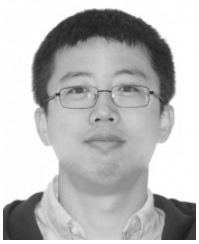

Yanjun Su received the B.E. degree in surveying and mapping engineering from the China University of Geosciences, Beijing, China, in 2009, the M.S. degree in geographic information science from the Institute of Geographic Sciences and Natural Resources Research, Chinese Academy of Sciences, Beijing, China, in 2012, and the Ph.D. degree in environmental systems from the University of California at Merced, Merced, CA, USA, in 2017.

He is currently an Associate Professor with the Institute of Botany, Chinese Academy of Sciences, Beijing. His current research interests include applying geographic information science and remote sensing to understand the influence of anthropogenic activities and global climate change on terrestrial ecosystems with a particular emphasis on the terrestrial carbon cycle, terrestrial biodiversity, energy balance, and land-use/land-cover change.

Tianyu Hu received the B.S. degree in ecology from China Agricultural University, Beijing, China, in 2008, and the Ph.D. degree from the Institute of Botany, Chinese Academy of Sciences, Beijing, in 2014.

He is currently an Assistant Professor with the Institute of Botany, Chinese Academy of Sciences. His current research interests include using LiDAR technology and dynamic vegetation model to understand forest ecosystem, especially in forest structure, function, and biodiversity.

Guangcai Xu received the B.E. degree in geographic information science and the M.S. degree in forest management from Nanjing Forestry University, Nanjing, China, and the Ph.D. degree in forest management form the Chinese Academy of Forestry, Beijing, China.

His current research interests include applying LiDAR technology (including Airborne, unmanned aerial vehicle, and terrestrial) to resolve the practical problems in forestry survey, planning, management, and dynamic inspections.

Qinghua Guo received the B.S. degree in environmental science and the M.S. degree in remote sensing and geographic information system (GIS) from Peking University, Beijing, China, in 1996 and 1999, respectively, and the Ph.D. degree in environmental science from the University of California at Berkeley, Berkeley, CA, USA, in 2005.

He is currently a Professor with the Institute of Botany, Chinese Academy of Sciences, Beijing. He is also an Adjunct Professor and a member of the Founding Faculty, School of Engineering, University of California at Merced, Merced, CA, USA. His current research interests include GIS and remote sensing algorithm development and their environmental applications, such as object-based image analysis, geographic one-class data analysis, and LiDAR data processing.